ionization of the modified Tyr, in excellent agreement with the value of 7.7 measured spectrophotometrically.[15] A similar analysis of kinetic data for the CPA-catalyzed hydrolysis of *O*-(*trans*-cinnamoyl)-L-β-phenyllactate gave an estimated value of pK_a = 8.2 for the ionization of unmodified Tyr-248. It seems probable, therefore, that the pK_a values in the vicinity of 8 measured for the binding of (−)-**1** to Zn(II) and Co(II) CPA represent the ionization of the phenolic hydroxyl of Tyr-248. While the stereochemical studies[4] on the enolization of (−)-**1** catalyzed by CPA as well as the pH dependency of k_{cat} for this process argue against the involvement of the phenol or phenoxide forms of Tyr-248 in a catalytic step, the X-ray study of the CPA–(−)-**1** complex[7,8] shows that the Tyr-248 residue is in close proximity to the bound substrate. As has been proposed for some ester substrates ("nonspecific" substrates[11,16]) , coordination of the Tyr-248 phenolate group to the active-site zinc may result in effective intramolecular competitive inhibition, causing poorer binding of (−)-**1** to CPA as the pH is raised in the vicinity of pH 8.

In addition to Glu-270 and Tyr-248, the two enzyme-bound moieties in close proximity to the substrate (−)-**1** in its complex with CPA are the zinc ion and the Arg-145 residue. Kinetic studies on the arsanilazo Tyr-248 CPA-catalyzed hydrolysis of **2** have been interpreted to indicate that the p*K* value of 9.1 calculated for the descending limb of the pH profile of k_{cat}/K_m corresponds to the ionization of the zinc-bound water at the active site,[9] a conclusion that is in agreement with the results of the spectrophotometric titration of this modified enzyme.[15] In view of the present observations that the pH dependency of K_I for the binding of (−)-**1** to both Zn(II) and Co(II) CPA appears to depend not only on an enzyme-bound group with $pK_a \simeq 8$ but also on one with $pK_a > 9$, a reasonable interpretation of our findings with (−)-**1** is that ionization of the zinc- (or cobalt-) bound water at the active site retards the formation of the CPA–(−)-**1** complex.

In summary, from measurements on the pH dependency of the parameter k_{cat} for the Zn(II) and Co(II) CPA catalyzed deuterium–hydrogen exchange of (−)-**1**-d_2, we have obtained a pK_a value of approximately 6 for the ionization of the catalytically important γ-carboxyl of Glu-270.[17] From a study of the pH dependency of K_I, the inhibition constant for (−)-**1** acting as an inhibitor in the Zn(II) and Co(II) CPA catalyzed hydrolysis of **2**, we assign the observed pK_a values of $\simeq$8 and >9 to the phenolic hydroxyl of Tyr-248 and to the active-site metal ion bound water.[18]

Acknowledgment. We are grateful to the National Institute of Arthritis, Metabolic and Digestive Diseases for support of this research. The NMR instruments used in this work were partly financed by the National Cancer Institute (PHS CA-14599) via the University of Chicago Cancer Research Center and by the National Science Foundation. The helpful comments of Dr. N. T. Nashed are acknowledged with gratitude.

Registry No. (−)-**1**, 68973-52-4; (−)-**1**-d_2, 84712-44-7; CPA, 11075-17-5; *O*-(*trans*-*p*-chlorocinnamoyl)-L-β-phenyllactate, 61556-61-4; Glu, 56-86-0; Tyr, 60-18-4.

(15) Johansen, J. T.; Vallee, B. L. *Proc. Natl. Acad. Sci. U.S.A.* **1973**, *70*, 2006.
(16) Carson, F. W.; Kaiser, E. T. *J. Am. Chem. Soc.* **1966**, *88*, 1212.
(17) The observation that the K_I (K_m) value for the complex of CPA with (−)-**1**-d_2 is nearly independent of pH between pH 5 and 6.5, together with the p*K* value of approximately 6 determined from the pH dependency of k_{cat}, suggest that a p*K* of about 6 also controls the pH dependency of k_{cat}/K_m for (−)-**1**-d_2 in acidic solution. It appears, therefore, that the binding of (−)-**1**-d_2 does not cause a perturbation of the p*K* of Glu-270.
(18) Address correspondence to E. T. Kaiser at the Laboratory of Bioorganic Chemistry and Biochemistry, The Rockefeller University, New York, New York 10021.

Out-of-Plane Deformation Modes in the Resonance Raman Spectra of Metalloporphyrins and Heme Proteins

Sunhee Choi and Thomas G. Spiro*

Contribution from the Department of Chemistry, Princeton University, Princeton, New Jersey 08544. *Received August 2, 1982*

Abstract: The systematics of low-frequency (<1000 cm^{-1}) resonance Raman (RR) spectra have been explored for a series of iron–porphyrin complexes and myoglobin derivatives, with the aid of ^{54}Fe substitution and deuteration at the methine and vinyl (for protoporphyrins) carbon atoms. Evidence is presented for activation of several out-of-plane deformation modes. These include modes assigned to methine hydrogen (~840 cm^{-1}) and carbon (~300 cm^{-1}) motions, pyrrole folding (425–510 cm^{-1}), and two ^{54}Fe-sensitive modes at ~250 and ~380 cm^{-1}, suggested to be coupled pyrrole tilting and substituent deformation. These are superimposed on the in-plane skeletal deformation Raman modes. Protoporphyrin complexes also show RR activation of in-plane IR modes and a pair of modes (~412 and ~290 cm^{-1}) associated with deformations of the vinyl groups. Activation mechanisms for the out-of-plane modes are discussed. The myoglobin spectra suggest that these modes are sensitive to heme–globin interactions.

Metalloporphyrins and heme proteins display Raman bands in the 1000–1700-cm^{-1} region that are strongly enhanced in resonance with the dominant Q (α and β) and B (Soret) electronic transitions.[1] These arise from in-plane ring modes which are coupled to the π–π* excitations. They have been extensively analyzed and correlated with porphyrin structure.[1-5] Enhancements are less marked for modes below 1000 cm^{-1} since these involve ring deformations and stretching of bonds to the central metal ion and are not as strongly coupled to the π–π* excitations; in addition there is a natural falloff of Raman intensity with decreasing vibrational frequency, if all other factors are equal.[6] This region is nevertheless of much interest because the bonds to the central metal ion are directly affected by chemical changes at the heme group. Under some conditions, good quality spectra

(1) Spiro, T. G. In "Iron Porphyrins"; Lever, A. B. P., Gray, H. B., Eds.; Addison-Wesley: Reading, MA, 1982; Part II, pp 89–152.
(2) Kitagawa, T.; Ozaki, Y.; Kyogoku, Y. *Adv. Biophys.* **1978**, *11*, 153.
(3) Warshel, A. *Annu. Rev. Biophys. Bioeng.* **1977**, *6*, 273.
(4) Felton, R. H.; Yu, Nai-Teng In "The Porphyrins"; Dolphin, D., Ed.; Academic Press: New York, 1978, Vol. II, Part A, pp 347–388.
(5) Asher, S. A "Methods in Enzymology, Hemoglobin Part, A"; Eraldo, L. B., Bernardi, E., Cheancone, Eds.; Academic Press: New York, 1981.
(6) Tang, J.; Albrecht, A. C. In "Raman Spectroscopy"; Szymanski, H. A., Ed.; Plenum Press: New York, 1970; Vol. 2, p 33.

0002-7863/83/1505-3683$01.50/0

can be obtained. Considerable progress has been made in identifying metal–axial ligand stretching modes via isotope substitution.[1] The rest of the low-frequency bands, which are often numerous, have not been thoroughly analyzed, although there have been frequent observations that these bands are sensitive, in varying degree, to chemical alterations of the heme group. A beginning has been made via the assignment of the in-plane modes of NiOEP[7,8] (OEP = octaethylporphyrin), including several in the low-frequency region, and the subsequent analysis of the NiPP[9] (PP = protoporphyrin IX) and heme[10] in-plane modes, including low-frequency vinyl modes.

In the present work we examine closely the low-frequency resonance Raman (RR) spectra of a series of heme complexes, using vinyl and methine deuteration shifts, as well as $^{54/56}$Fe shifts, to make assignments. Out-of-plane porphyrin RR modes are identified for the first time, and mechanisms for their enhancement are discussed.

Experimental Section

Meso-deuterated protoporphyrin IX (PP) was prepared by a modification of literature methods.[11,12] For convenience in purification and metal insertion, PP dimethyl ester was used as a starting material instead of the free acid. NMR established that the meso positions were deuterated to the extent of 90%, leaving the vinyl group intact. Insertion of Fe into PP-d_4 dimethyl ester was carried out in dimethylformamide (DMF).[13] The resulting [Fe^{III}PP(DME)-d_4]Cl was purified by chromatography on Al_2O_3 and hydrolyzed to [Fe^{III}PP]Cl. Meso-deuterated octaethylporphyrin (OEP) was prepared[14] by stirring OEP in 90 wt % D_2SO_4/D_2O for 12 h at room temperature. NMR spectroscopy showed 93% meso deuteration. ^{54}Fe–PP(DME) or ^{54}Fe–OEP was prepared by a modified acetate method.[13] To refluxing concentrated acetic acid under N_2 gas was added 33 mg of ^{54}Fe powder (17%, Oak Ridge National Lab), followed by a minimum amount of concentrated HCl, until all the ^{54}Fe powder was dissolved (the solution became yellow). PP(DME) or OEP (80 mg), dissolved in a minimum amount of pyridine was then added to the refluxing solution. After 15 min of refluxing, no fluorescence associated with porphyrin free base, was detectable. The solution was cooled and [^{54}Fe^{III}PP(DME)]Cl or [^{54}Fe^{III}OEP]Cl was separated out with CH_2Cl_2. Hemin chloride deuterated at the C_α or C_β vinyl carbon atoms was provided by Professor K. M. Smith; the method of preparation is described elsewhere.[15] Reconstitution of myoglobin (Mb) with modified hemes was carried out by standard methods.[16] The vinyl deuterated Mb samples were provided by Professor G. N. La Mar.

The protoporphyrin and mesoporphyrin complexes were prepared as described in ref 10. [(ImH)$_2$Fe^{III}OEP]$^+$ was prepared by dissolving [Fe^{III}OEP]Cl and excess imidazole in DMF (DMF = dimethylformamide). For the preparation of [(CN)$_2$Fe^{III}OEP]$^-$, concentrated aqueous KCN was added to a DMF solution of [Fe^{III}OEP]Cl$^-$.

Resonance Raman spectra were obtained as described elsewhere.[17] The data were collected digitally with a MINC computer. The spectra were smoothed with a Gaussian filter to obtain accurate peak frequencies.

Results

RR spectra below 1000 cm^{-1} were studied for protoheme complexes representing the major oxidation, spin, and ligation states found in heme proteins: [(ImH)$_2$Fe^{III}PP]$^+$ (6-coordinate, low spin; ImH = imidazole), (ImH)$_2$Fe^{II}PP (6-coordinate, low spin), (2-MeImH)Fe^{II}PP (5-coordinate, high spin; 2-MeImH = 2-methyl imidazole), ClFe^{III}PP (5-coordinate, high spin) and [(Me$_2$SO)$_2$Fe^{III}PP]$^+$ (6-coordinate, high spin; Me$_2$SO = dimethyl sulfoxide). Low-spin dicyano adducts were also examined. The effects of ^{54}Fe substitution and of meso and vinyl deuteration on the observed frequencies were determined. Analogous mesoporphyrin (MP) and octaethylporphyrin (OEP) complexes were also examined. PP complexes were studied in water or in aqueous detergent (SDS or TX-100) solution, while OEP complexes were dissolved in benzene or dimethylformamide (DMF). The aqueous PP complexes show split Soret absorption bands indicative of aggregation. The splitting altered the RR enhancement and indeed proved useful in detecting certain Raman bands (vide infra), but there were no changes in frequency beyond 1–2 cm^{-1}. Adding detergents to these solutions inhibited aggregation and produced essentially the same absorption and RR spectra as seen in organic solvents. Most of the spectra were obtained with 4131- or 4579-Å excitation, since resonance with the B (Soret) band gave the greatest enhancement of most of the low-frequency modes. The frequency data are summarized in Table I. Also listed in the table are frequencies reported by Spaulding et al.[18] for a crystalline form of NiOEP known to contain a ruffled prophyrin ring with D_{2d} symmetry.[19]

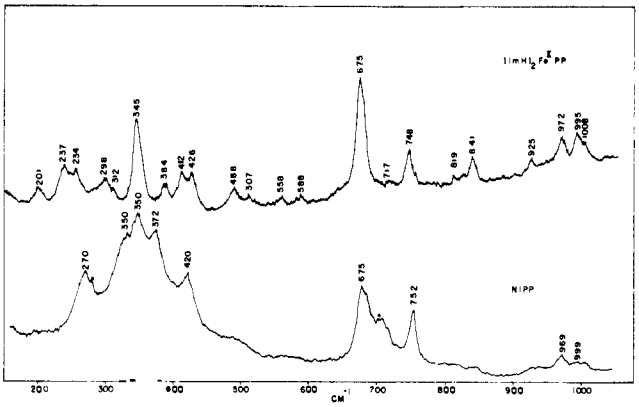

Figure 1. B-band-excited low-frequency RR spectra of (ImH)$_2$Fe^{II}PP (~1 mM in H_2O with ~1 M ImH; λ_0 = 4579 Å) and of NiPP (~1 mM in CH_2Cl_2; solvent bands are marked with asterisks; λ_0 = 4131 Å). Spectral slit width, 5 cm^{-1}.

Discussion

A. Fe–Axial Ligand Stretches. The Fe–2MeImH stretch in 5-coordinate (2MeImH)Fe^{II}PP has been assigned via ligand perdeuteration[20] and $^{54/56}$Fe[21] frequency shifts to the relatively strong RR band seen at 220 cm^{-1} in water and ~208 cm^{-1} in organic solvents and in aqueous detergents. This band has alternatively been assigned to Fe–N(pyrrole) stretching,[22] but its appreciable ^{15}N(pyrrole) shift (1.5 cm^{-1})[23,24] is more likely due to mixing with a nearby out-of-plane tilting mode of the pyrrole rings (vide infra). For ClFe^{III}OEP (OEP = octaethylporphyrin), Ogoshi et al.[25] assigned ν_{Fe-Cl} to a 357-cm^{-1} infrared band; this frequency is obscured in the RR spectrum by a strong porphyrin band at 345 cm^{-1}. The symmetric (ImH)–Fe–(ImH) stretch is now assigned on the basis of its imidazole ^{15}N[24] and perdeuteration[26] shift to a weak Soret-enhanced RR band at ~200 cm^{-1} for *both* [(ImH)$_2$Fe^{III}PP]$^+$[26] and (ImH)$_2$Fe^{II}PP,[24,26] close to the corresponding py–Fe–py (py = pyridine) frequency 179 cm^{-1}, of (py)$_2$Fe^{II}MP.[27] The assymmetric stretch of

(7) Kitagawa, T.; Abe, M.; Ogoshi, H. *J. Chem. Phys.* **1978**, *69*, 4516.
(8) Abe, M.; Kitagawa, T.; Kyogoku, Y. *J. Chem. Phys.* **1978**, *69*, 4526.
(9) Choi, S.; Spiro, T. G.; Langry, K. C.; Smith, K. M. *J. Am. Chem. Soc.* **1982**, *104*, 4337–4344.
(10) Choi, S.; Spiro, T. G.; Langry, K. C.; Smith, K. M.; Budd, D. L.; La Mar, G. N. *J. Am. Chem. Soc.* **1982**, *104*, 4345–4351.
(11) Kenner, G. W.; Smith, K. M.; Sutton, M. J. *Tetrahedron Lett.* **1973**, 1303–1306.
(12) Nagai, K.; Welborn, C.; Dolphin, D.; Kitagawa, T. *Biochemistry* **1980**, *9*, 4755.
(13) Buchler, J. W. In "Porphyrins and Metalloporphyrins"; Smith, K. N., Ed.; American Elsevier: New York, 1976; pp 157–231.
(14) Bonnett, R.; Stephenson, G. F. *Proc. Chem. Soc., London* **1964**, 291.
(15) Budd, D. L.; La Mar, G. N.; Langry, K. C.; Smith, K. M.; Nayyu-Mazliu, R. *J. Am. Chem. Soc.* **1979**, *101*, 6091.
(16) Teale, F. W. J. *Biochim. Biophys. Acta* **1959**, *35*, 543.
(17) Spiro, T. G.; Stong, J. D.; Stein, P. *J. Am. Chem. Soc.* **1979**, *101*, 2648.
(18) Spaulding, L. D.; Chang, C. C.; Yu, N.-T.; Felton, R. H. *J. Am. Chem. Soc.* **1975**, *97*, 2517.
(19) Meyer, E. F., Jr. *Acta Crystallogr., Sect. B* **1972**, *28*, 2162.
(20) Kincaid, J.; Stein, P.; Spiro, T. G. *Proc. Natl. Acad. Sci. U.S.A.* **1979**, *76*, 549, 4156.
(21) Kitagawa, T.; Nagai, K.; Tsubaki, M. *FEBS Lett.* **1979**, *104*, 376.
(22) Desbois, A.; Lutz, M.; Banerjee, R. *Biochemistry* **1979**, *18*, 1510.
(23) Desbois, A.; Momenteau, M.; Loocks, B.; Lutz, M. *Spectrosc. Lett.* **1980**, *14*, 257–269.
(24) Desbois, A.; Lutz, M. *Biochim. Biophys. Acta* **1981**, *671*, 168–176.
(25) Ogoshi, H.; Watanabe, E.; Yoshida, Z.; Kincaid, J.; Nakamoto, K. *J. Am. Chem. Soc.* **1973**, *95*, 2845.
(26) Mitchell, M.; Choi, S.; Spiro, T. G., manuscript in preparation.

Table I. RR Frequencies (cm^{-1}) below 1000 cm^{-1} for PP, OEP, and/or MP Complexes

mode[a]			NiOEP			$(1mIl)_2Fe^{III}$		$(1mH)_2Fe^{II}$		$ClFe^{III}$		$(Me_2SO)_2Fe^{III}$	(2-MeImH)Fe^{II}		frequency shifts[c]	
			D_{4h}	D_{2d}[b]	NiPP	PP	MP	PP	MP	PP	MP	PP	PP	MP	Δd_{4m}	$\Delta^{54}Fe$
		γCH_2			999	1008		1008[e]					1005			
ν_{45}	E_u	C_aN			999	997	1001	995					999	989	17	
$\nu_{32} + \nu_{35}$	A_{1g}		963	964	969	972	981	972	973				982		18	
ν_{46}	E_u	C_bS		943		951	951	925	939				921	927	*d*	
		γC_mH		844		845	846	841							*d*	
ν_6	A_{1g}	$\delta C_aC_mC_a$	806	803	805	804	805	819	806	806	800	786	787	788		
ν_{32}	B_{2g}	δC_bS	782		782	791		791								
$\nu_{33} + \nu_{34}$	A_{1g}		770	774	770		774	776	778	756	760	788				
ν_{16}	B_{1g}	δC_aNC_a	751	751	752	749	749	748	744	722	733		752	750	68	
ν_{47}	E_u	C_bS				714	712	717		694	717		714	712	67	
ν_7	A_{1g}	δC_bC_aN	675	675	675	677	677	675	675	675	675	677	676	673	67	
ν_{48}	E_u	δC_bS		609		605		588					585			
ν_{49}	E_u	$\delta C_aC_bC_b$		551		561		558		555			548		12	
		pyr fold		526		510	525	507[f]					510			
		pyr fold		481		495	495	488[f]		492	489	495	495			
		pyr fold				425	395	426		410	425					
		$\delta C_bC_\alpha C_\beta(1)$			420	419		412[g]		415		414	410			
		γC_bS						384		380	381					2
$2\nu_{35}$			361		372	380	379		381	373		375	374	379	2	
ν_8		δC_bS	345	350	350	349	349	345	345	345	351	344	345	345	1-5	
		$\delta C_bC_\alpha C_\beta(2)$			330	312		312[g]		324			326			
		γC_mC_a				296	290	298	306	312			303	286	7	1-2
ν_9		δC_bS	264	283	270	276	265	263	261	266	261	270				
		pyr tilt						254	248				255	255		2-3
			226		220	236	240	237	235							
		ν_{Fe-Im}				199	200	201	201							6

[a] Mode numbers and skeletal assignments follow Abe et al.[8] [b] Frequencies are taken from ref 18. [c] Downshifts observed upon meso deuteration and upshift observed on ^{54}Fe substitution. [d] These bands disappear upon meso deuteration. [e] Disappears for $-d_{2\beta}$. [f] Downshifts 6 cm^{-1} for $-d_\alpha$. [g] Downshifts 10 cm^{-1} for $-d_{2\beta}$.

Table II. Out-of-Plane Modes of a Metalloporphine, Calculated with a Semiempirical Force Field (QCFF/PI)

sym	frequency, cm^{-1}	description[b]	sym	frequency, cm^{-1}	description
E_g	1064	γH	E_g	556	γC
B_{1u}	1063	γH	B_{2u}	541	γC
B_{2u}	1062	γH	B_{1u}	414	γm
A_{2u}	855	γH	E_g	373	γC
A_{2u}	852	γH(m)	A_{1u}	290	γC
E_g	851	γH(m)	A_{2u}	278	γm
A_{2u}	788	γC	E_g	172	γm
B_{1u}	788	γH	A_{2u}	153	γM
E_g	787	γH	B_{2u}	146	γN
B_{1u}	594	γC	E_g	130	γN
E_g	591	γC	B_{1u}	77	
A_{2u}	581	γC	B_{2u}	55	γa
A_{1u}	579	γC	A_{2u}	54	γM

[a] From ref 29. [b] γy designates deformation around atom; y = H (pyrrole H), and H(m) (methine H), C (pyrrole C), m (methine C), a (a position C), N (pyrrole N), M (metal).

Table III. Local Mode Contributions to the Out-of-Plane Normal Modes of a D_{4h} OEP-Type Metalloporphyrin, with Point Mass Pyrrole Substituents S

local mode[a]	symmetry				
	A_{1u}	A_{2u}	B_{1u}	B_{2u}	E_g
γC_mH		1	1		1
pyr fold (s)		1		1	1
pyr fold (as)	1		1		1
γC_bS	1	1	1	1	2
γC_aC_m		1	1		1
pyr tilt		1		1	1
pyr swivel	1		1		1
pyr transl		(1)[b]		1	(1)[c]
γ_{NM}		1			
Out-of-Plane Vibrational Representation	3	6	5	4	8

[a] See Figure 5 for descriptions. [b] Molecular translation (z). [c] Molecular rotations (R_x, R_y).

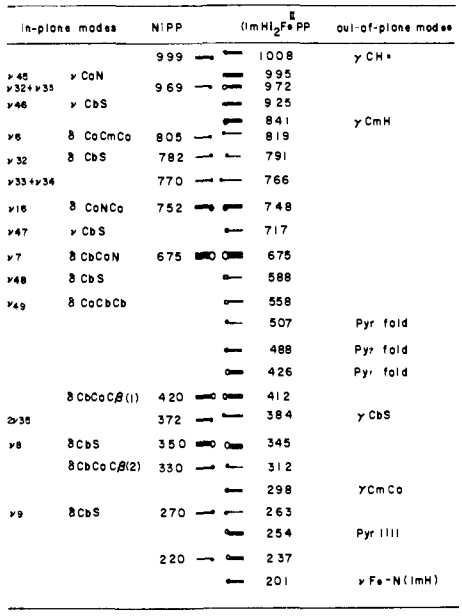

Figure 2. Schematic diagram of the RR bands of NiPP and $(ImH)_2Fe^{II}PP$, with proposed assignments of the in-plane (left) and out-of-plane (right) modes. The thickness of the lines indicates the relative intensities of the bands, at the wavelengths of maximum enhancement. The 841- and 748-cm^{-1} bands (filled circles) are depolarized, and the remaining bands (open circles) are polarized.

$[(ImH)_2Fe^{III}OEP]^+$ has been identified at 377 cm^{-1} in the IR spectrum.[25] For $[(Me_2SO)_2Fe^{III}PP]^+$ no candidates for axial modes have been observed; all RR bands are assignable to porphyrin modes. Likewise no axial modes have been detected for dicyano complexes of Fe^{III} or Fe^{II} porphyrins.

Asher and Schuster[28] have assigned $Mb^{III}F$ bands at 462 and 422 cm^{-1} to Fe–F stretching (the lower frequency mode being suggested to be associated with H bonding of a fraction of the F^- ligands to water molecules at a partially occupied site), and Desbois et al.[22] showed the 462-cm^{-1} mode to be ^{54}Fe-sensitive, as expected for Fe–F stretching. Neither of these modes is observed at exact Soret resonance, 4131 Å (see Figure 14). Nearby modes are seen at 472 and 442 cm^{-1}, but these are pyrrole deformation modes, as shown by their vinyl deuteration shifts (vide infra).

B. In-Plane Modes: Vinyl and E_u Modes. Figure 1 compares B-band-excited RR spectra below 1000 cm^{-1} for $(ImH)_2Fe^{II}PP$ and NiPP. The assignments are summarized in Figure 2. For NiPP, they have been developed in our previous study;[9] the additional assignments for $(ImH)_2Fe^{II}PP$ are discussed in this section and the succeeding ones. Figure 3 shows the influence of deuteration at the meso carbon atoms and at the vinyl C_α or C_β atoms on the $(ImH)_2Fe^{II}PP$ RR spectrum.

The bands between 1000 and 675 cm^{-1} arise chiefly from in-plane ring deformation modes.[8] Some of them are weak with B-band excitation but are seen clearly at 5145 Å near the Q_1 absorption band. The NiPP RR band at 999 cm^{-1} corresponds to an E_u mode (ν_{45}) of NiOEP,[8] based on its meso-d_4 shift;[9] several E_u modes are activated in PP RR spectra, via the asymmetrically disposed vinyl substituents.[9] In addition the 999-cm^{-1} band has a contribution from vinyl $C_\alpha H$ out-of-plane wagging, $\gamma_{CH=}$, as shown by its loss of intensity upon C_α deuteration.[9] In the $(ImH)_2Fe^{II}PP$ spectrum, $\gamma_{CH=}$ is a clear shoulder (1008 cm^{-1}) on the 995-cm^{-1} band, which disappears on C_α deuteration (Figure 3).

There are additional weak bands, at 925, 717, 588, and 557 cm^{-1}, which correspond to E_u modes (ν_{46-49})[8] of NiOEP, showing similar meso-deuteration shifts (Figure 3). Apparently, they are activated more effectively by $(ImH)_2Fe^{II}PP$ (and in some cases

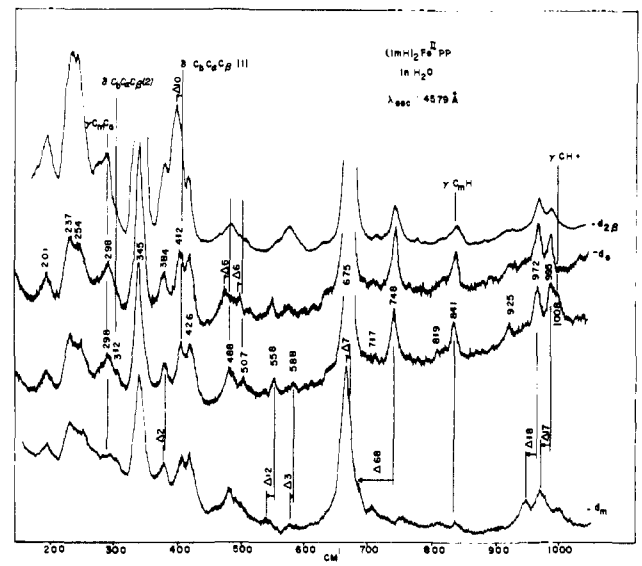

Figure 3. RR spectra $(ImH)_2Fe^{II}PP$ (as in Figure 1), showing the effects of deuteration at the vinyl C_β ($-d_{2\beta}$) or C_α ($-d_\alpha$) atoms, or at the meso carbon atoms ($-d_m$).

by the other iron complexes—see Table I) than by NiPP, for which they cannot be detected above the background (Figure 1). It is of interest that bands corresponding to ν_{46}, ν_{48}, and ν_{49} have also been seen in the RR spectrum of the D_{2d} form of NiOEP (Table I).[18]

In the 350-cm^{-1} region, both NiOEP and NiPP, and all the complexes included in this study, show a prominent pair of bands assigned to a Fermi resonance between an A_{1g} mode, ν_8, and the overtone of a mode at half the frequency, probably ν_{35} (B_{2g}).[8] Consistent with the proposed Fermi interaction, the intensity distribution between the two bands varies from one complex to another, although the lower freuency band at ~345 cm^{-1} is usually the more intense and therefore has the major ν_8 contribution. Flanking this doublet, NiPP, but not NiOEP, has a pair of bands at 420 and 330 cm^{-1}, both of which shift substantially upon C_β, but not C_α, vinyl deuteration and are assigned[9] to in- and out-of-phase bending of the vinyl groups, $\delta_{C_\beta C_\alpha C_\beta}$. The higher of these two modes is seen in all the iron PP complexes at 412–419 cm^{-1}. The lower one appears to be shifted down to ~310 cm^{-1} and merges in a broad band with another mode at ~300 cm^{-1}, which is believed (vide infra) to be an out-of-plane mode. The high-frequency part of the 305-cm^{-1} envelope loses intensity upon C_β deuteration, while the low-frequency part loses intensity upon C_m deuteration (see Figure 3).

There are three bands near 250 cm^{-1}, whose relative intensities vary with excitation wavelength, even in the vicinity of the Soret band. For example, aqueous $(ImH)_2Fe^{II}PP$ shows bands at 237 and 254 cm^{-1} with λ_0 = 4579 Å but at 237 and 263 cm^{-1} with λ_0 = 4131 Å. In several cases (Table I) only one or two of this trio of bands have been observed. The band at ~255 cm^{-1} is assignable to out-of-plane pyrrole tilting (vide infra), while the flanking bands are probably in-plane modes. One in-plane mode from each of the symmetry classes is expected in this region, according to the calculations of Abe et al.[8] They assign the A_{1g} mode to a weak band at 226 cm^{-1} in the spectrum of NiOEP; another band, at 264 cm^{-1}, appears stronger in our spectrum.[9] Since the band near 270 cm^{-1} is usually the stronger of the pair, we suggest it to be the lowest frequency A_{1g} mode, leaving a B_{1g}, B_{2g}, or A_{2g} assignment for the ~230-cm^{-1} band. (Its intensity is too low to permit polarization measurements.)

C. Out-of-Plane Modes: Compositions and Enhancement Mechanisms. Evidence is presented below for the appearance of several out-of-plane modes in Fe-porphyrin RR spectra. Since these modes do not appear to have been discussed elsewhere, we present a brief analysis of their composition and enhancement mechanisms. Warshel and Lappicirella[29] have recently used a semiempirical force field (QCFF/P1) to calculate both in- and

(27) Wright, P. G.; Stein, P.; Burke, J. M.; Spiro, T. G. *J. Am. Chem. Soc.* **1979**, *101*, 3531.
(28) Asher, S. A.; Schuster, T. M. *Biochemistry* **1979**, *18*, 5377.

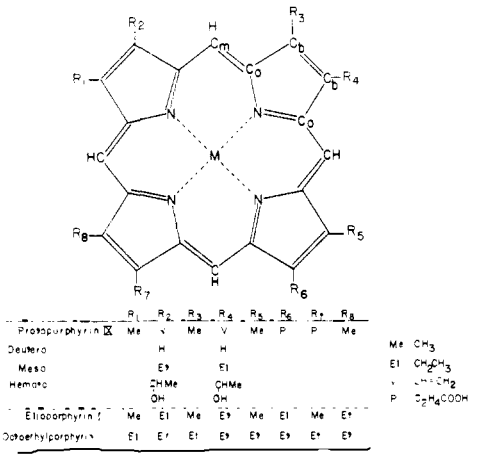

Figure 4. Structural diagram of a metalloporphyrin, with the substituent patterns for several common types.

out-of-plane modes of a metalloporphine; their out-of-plane frequencies are listed in Table II. Porphine differs from physiological-type prophyrins in having H atoms instead of carbon substituents attached to the pyrrole C_b atoms; the out-of-plane frequencies of the H atoms are, of course, much higher than those of the heavy substituents.

We first consider a planar metalloporphyrin with no axial ligands, and eight equivalent point mass substituents, S, attached to the pyrrole C_b atoms (Figure 4). This is the same model as was used for the in-plane analysis of NiOEP.[8] The 37-atom molecule has 34 out-of-plane vibrations, classified as

$$\Gamma_{oop} = 3A_{1u} + 6A_{2u} + 5B_{1u} + 4B_{2u} + 8E_g$$

It is instructive to categorize these modes according to the local motions of the structural elements making up the molecule, i.e., the C_mH methine bridges, the pyrrole rings, with their C_bS substituents, and the central metal atom. The local out-of-plane motions are illustrated in Figure 5, and their contributions to the symmetry blocks are listed in Table III.

The C_mH wags, expected[30] near 850 cm^{-1}, are the only modes involving hydrogen motions and are far above the other modes in frequency. Next in order of expected frequency are the out-of-plane deformations of the relatively rigid pyrrole rings. There are two folding modes of a planar pyrrole ring (Figure 5), which are symmetric and antisymmetric with respect to the 2-fold axis. In isolated five-membered heterocycles, these occur in the 400–600-cm^{-1} range.[30] Warshel and Lappicirella[29] calculate a group of six modes in this region (Table II) which can be identified with pyrrole distortions (six are expected, A_{1u}, A_{2u}, B_{1u}, B_{2u}, $2E_g$; Table III). The remaining modes are all expected to be below 400 cm^{-1}, and the local motions are certain to be more or less coupled. The addition of axial ligands to the metalloporphyrin model introduces in- and out-of-phase ν_{M-L} stretching modes, of A_{1g} and A_{2u} symmetry. The out-of-phase stretch can mix with the porphyrin A_{2u} modes.

Among all the out-of-plane modes only the A_{1g} ν_{M-L} stretch can be enhanced via A-term[6,31] (Franck–Condon) RR scattering as long as the symmetry remains D_{4h}. The eight E_g out-of-plane modes are Raman active, but since they are non-totally symmetric, they must be activated by a B term[6,31] (vibronic) mechanism. This mechanism requires that they be effective in mixing in- and out-of-plane electronic transitions ($E_uA_{2u} = E_g$). An example of E_g activation is described in the next section.

If the symmetry is lowered from D_{4h}, then additional possibilities arise. In particular, if the symmetry is lowered by destruction of the porphyrin mirror plane, e.g., by inequivalent axial ligands and/or out-of-plane displacement of the metal atom, then the A_{2u} modes transform as A_1, under the resulting C_{4v} symmetry. Thus A-term activation of infrared modes can be expected when the two sides of the porphyrin ring are not equivalent. Out-of-plane electronic transitions are not required for this mechanism. Resonance via an in-plane transition is possible if the out-of-plane mode modulates the transition (i.e., if the out-of-plane motion alters the in-plane electron distribution, thereby changing the in-plane transition probability). RR activation of several A_{2u} modes is described below.

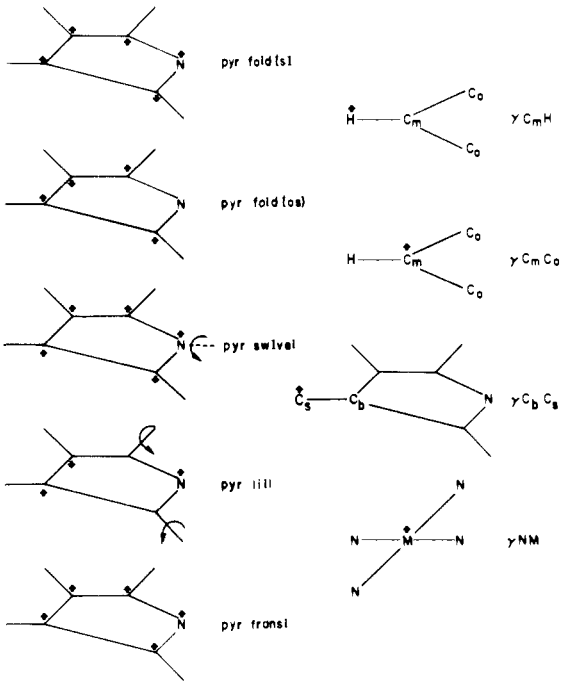

Figure 5. Schematic diagram for local out-of-plane motions of the porphyrin structural elements.

In C_{4v} symmetry, the remaining out-of-plane modes are also Raman active—$B_{1u} \rightarrow B_2(xy)$, $B_{2u} \rightarrow B_1(x^2 - y^2)$, $A_{1u} \rightarrow A_2(xy - yx)$ (the A_2 mode is antisymmetric)—but they all require a vibronic mixing mechanism for activation, involving in-plane electronic transitions; the situation is analagous to the activation of in-plane B_{1g}, B_{2g}, and A_{2g} modes in D_{4h} symmetry.[1] Thus, B_{1u}, B_{2u}, and A_{1u} modes are less likely to be observed, since they require both symmetry lowering and an in-plane vibronic mechanism.

If the mirror plane is retained but the axial symmetry is destroyed, i.e., via asymmetric peripheral substitutents, as in protoporphyrins, then all the in-plane vibrations classify as A, in the resulting C_s symmetry, and are potentially Franck–Condon active, while all the out-of-plane modes classify as B and require activation by mixing of in- and out-of-plane electronic transitions (AxB = B).

D. E_g Mode Enhancement. Upon excitation at 4579 Å, $(ImH)_2Fe^{II}PP$ shows a band at 841 cm^{-1}, which disappears upon meso deuteration (Figure 3). This frequency is characteristic of out-of-plane deformations of aromatic C–H bonds,[30] and Abe et al.[8] have assigned a 835-cm^{-1} infrared band of NiOEP, which shifts to 678 cm^{-1} upon meso deuteration (in the RR spectrum this frequency is obscured by an intense porphyrin mode, ν_7), to the A_{2u} γ_{C_mH} mode. The 841-cm^{-1} RR band, however, is depolarized and therefore assignable to E_g. The A_{2u} and E_g γ_{C_mH} modes are expected to be essentially degenerate, since the C_mH bonds are far apart; Warshel and Lappicirella[29] calculate them at 851–855 cm^{-1} (Table II).

The 841-cm^{-1} RR band is seen with appreciable intensity for $(ImH)_2Fe^{II}PP$ only with 4579-Å excitation and only for aqueous solution. In water, the 440 nm component of the split B band is close to the exciting line (Figure 6). If detergent is added, a single B band is seen, with λ_{max} = 413 nm, and the 841-cm^{-1} RR band is no longer observed, even when 4131-Å excitation is used, in exact resonance. We conclude that the E_g mode enhancement is due to vibronic coupling of a z-polarized electronic transition

(29) Warshel, A.; Lappicirella, A. *J. Am. Chem. Soc.* **1981**, *103*, 4664.
(30) Colthup, N. B.; Daly, L. H.; Weiberley, F. E. "Infrared and Raman Spectroscopy" 2nd ed.; Academic Press: New York, 1975, pp 275–277.
(31) Spiro, T. G.; Stein, P. *Annu. Rev. Phys. Chem.* **1977**, *28*, 501.

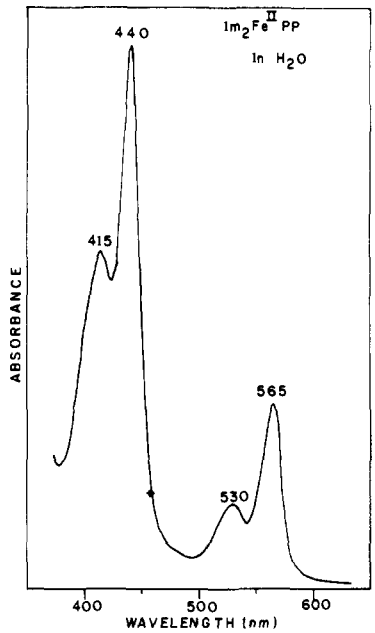

Figure 6. Absorption spectrum of aqueous $(ImH)_2Fe^{II}PP$, showing the split B band (415 and 440 nm), due to aggregation, and the position (arrow) of the 4579-Å excitation, where enhancement of the 841-cm^{-1} γ_{C_mH} vibration is specifically observed.

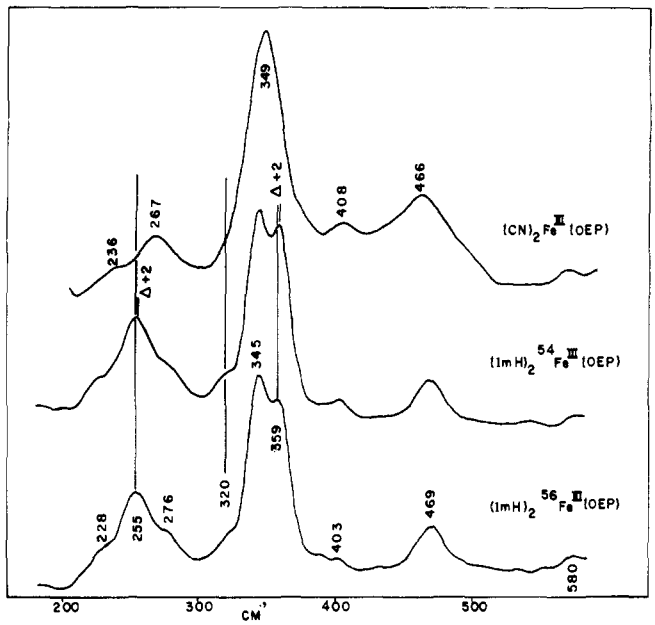

Figure 7. Low-frequency RR spectra of $[(ImH)_2Fe^{III}OEP]Cl$, its ^{54}Fe isotopic form, and of $K[(CN)_2Fe^{III}OEP]$, in DMF (~1 mM). Note the disappearance of the bands at 255, 320, and 359 cm^{-1} in the top spectrum.

near 4579 Å, which is itself too weak to be seen in the absorption spectrum, with the nearby component of the split (x,y-polarized) B transition. When the B band is as high as 413 nm, the coupling is weakened sufficiently to render the band unobservable.

The likeliest candidate for the z-polarized transition is porphyrin $\pi(a_{2u}) \rightarrow Fe\ d_{z^2}(a_{1g})$ charge transfer. The a_{2u} orbital has substantial electron density at the methine carbon atoms,[32] and out-of-plane C_m–H bending can therefore be effective in vibronic mixing. The situation is somewhat analogous to that found in pyrazine, in which RR enhancement is found for a C–H out-of-plane mode that mixes the $n \rightarrow \pi^*$ and $\pi \rightarrow \pi^*$ electronic transitions.[33] Makinen and Churg[34] have assigned the $a_{2u} \rightarrow d_{z^2}$ transition to polarized absorption bands observed in a number of heme proteins via oriented crystal spectroscopy. For $Mb^{II}CN$, which contains low-spin Fe^{II}, the transition was assigned at 475 nm, and similar energies were found for other heme proteins containing low-spin Fe^{II} or Fe^{III} (MbCO, MbO_2, $Mb^{III}CN$).[34] Occurrence of the $a_{2u} \rightarrow d_{z^2}$ transition near 4579 Å for $(ImH)_2Fe^{II}PP$ is therefore not unreasonable. (No examples of bis(imidazole) hemes were included in the protein crystal studies.) Alternatively, the z-polarized transition might be an out-of-plane intermolecular porphyrin transition associated with the aqueous aggregates in the sample.

E. A_{2u} Mode Enhancement. Figure 7 compares low-frequency RR spectra, with direct B-band excitation (4131 Å), of the dicyano and bis(imidazole) complexes of $Fe^{III}OEP$, and shows the effect of ^{54}Fe substitution in the bis(imidazole) complex. All of the features are polarized ($\rho \leq 0.3$). Two bands, at 255 and 359 cm^{-1}, are seen to shift up upon ^{54}Fe substitution. Both bands are absent in the $[(CN)_2Fe^{II}OEP]^-$ spectrum, as is a shoulder, at 320 cm^{-1}, on the strong 345-cm^{-1} band. The ^{54}Fe sensitivity of this shoulder is uncertain; Ogoshi et al.[24] report a 1-cm^{-1} ^{54}Fe upshift of an IR band at this frequency (319 cm^{-1}). The 320-cm^{-1} shoulder shifts down appreciably, by 10 cm^{-1}, upon meso deuteration of $[(ImH)_2Fe^{III}OEP]^+$ (spectrum not shown).

In D_{4h} symmetry the central atom cannot move in any g mode, but only in the u modes. The ^{54}Fe isotope sensitivity therefore identifies the 255- and 359-cm^{-1} bands with u vibrational modes. However, u modes are Raman inactive. Their appearance in the RR spectrum therefore implies that the molecular symmetry is lower than D_{4h}; in particular, the symmetry center must be lost.

This is a surprising result since $[(ImH)_2Fe^{III}OEP]^+$ has identical peripheral substituents, maintaining the 4-fold symmetry, and apparently identical axial ligands, which should maintain the porphyrin mirror plane. However, the crystal structure[35] of the chloride salt of the TPP analogue shows the two imidazole ligands to be decidely nonequivalent. The Fe–ImH bond lengths (1.957 and 1.991 Å) are significantly different; the longer bond is associated with an imidazole orientation that brings pyrrole N and imidazole H atoms into short nonbonded contact. In the crystal lattice, the imidazole orientations are presumably determined by packing forces and by H bonds from the N1 imidazole protons to the Cl^- counterions and to co-crystallized methanol molecules.[35]

In solution, these fixed restraints are absent, but H bonds to excess imidazole molecules are known to be important,[36] and the instantaneous structure may be asymmetric with respect to the porphyrin plane, thereby activating A_{2u} out-of-plane modes. This appears to be the only plausible explanation of the presence of ^{54}Fe-sensitive bands in the RR spectrum. It is strongly supported by the disappearance of these bands when imidazole is replaced by CN^-, which is less sterically demanding, and for which H bonding is unlikely to be important.

1. Pyrrole Tilting. We assign the 255-cm^{-1} band to a mode primarily involving concerted tilting of the pyrrole rings. The 1-cm^{-1} ^{15}N(pyrrole) downshift observed by Desbois et al.[22] for the 251-cm^{-1} RR band of $(ImH)_2Fe^{II}EP$ (EP = etioporphyrin) is consistent with this assignment, since pyrrole tilting would move the N atoms appreciably. RR activation of this mode is plausible linked to a mechanism involving loss of the porphyrin mirror plane via nonbonded contacts of the pyrrole N atoms with the imidazole H atoms; these contacts would most readily be accommodated by tilting of the pyrrole rings. The dipole moment generated by this mode is evidently small, since no band at this position is seen in the IR spectrum.[24]

A ^{54}Fe-sensitive band near 255 cm^{-1} has been observed for the following species (Figures 7–11): $[(ImH)_2Fe^{III}OEP]^+$, $(ImH)_2Fe^{II}PP$, (2-MeImH)$Fe^{II}PP$, Mb^{II}, $Mb^{III}F^-$ and $Mb^{III}ImH$

(32) Longuett-Higgins, H. C.; Rector, C. W.; Platt, J. R. *J. Chem. Phys.* **1950**, *18*, 1174.
(33) Ito, M.; Suzuka, I. *Chem. Phys. Lett.* **1975**, *31*, 467.
(34) Makinen, M. W.; Churg, A. K. In "Iron Porphyrins"; Lever, A. B. P., Gray, H. B., Eds.; Addison-Wesley: Reading, MA, 1982.
(35) Collins, D. M.; Countryman, R.; Hoard, J. L. *J. Am. Chem. Soc.* **1972**, *94*, 2066.
(36) Walker, F. A.; Lo, M.-W.; Ree, M. T. *J. Am. Chem. Soc.* **1976**, *98*, 5552.

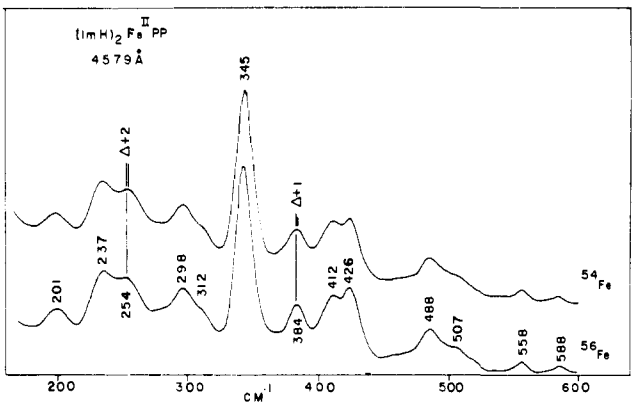

Figure 8. Low-frequency RR spectra (λ_0 = 4579 Å) of aqueous $(ImH)_2Fe^{II}PP$ and its ^{54}Fe form, both in ~1 mM concentration. Spectral slit width, 5 cm^{-1}.

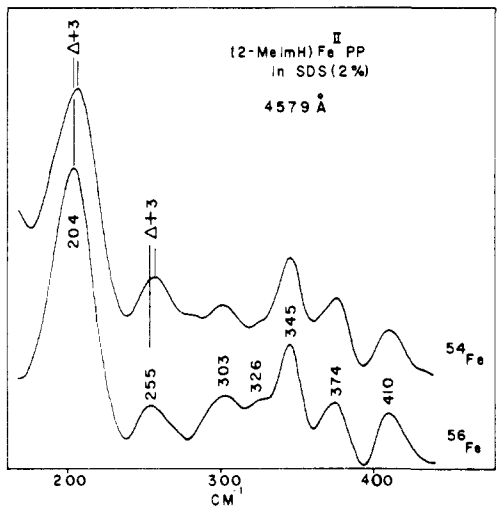

Figure 9. Low-frequency RR spectra (λ_0 = 4579 Å) of (2-MeImH)-$Fe^{II}PP$ and its ^{54}Fe form, both in 2% SDS aqueous detergent solution. Spectral slit width, 5 cm^{-1}.

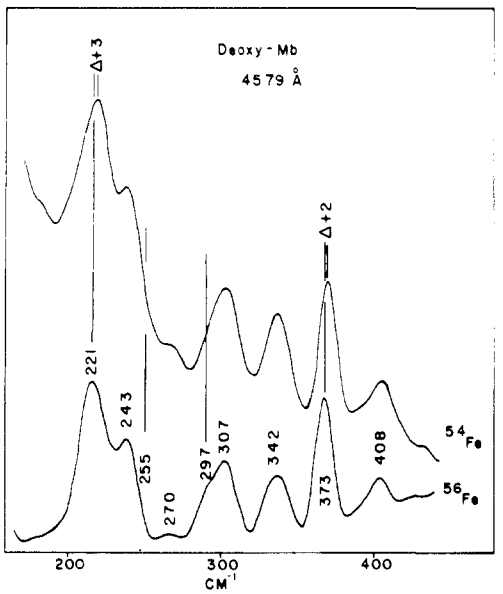

Figure 10. Low-frequency RR spectra (λ_0 = 4579 Å) of deoxyMb and deoxyMb reconstituted with $^{54}FePP$, both in ~0.05 mM bis-tris buffer (0.025 M, pH 6.5). Spectral slit width, 5 cm^{-1}.

(spectrum of the last species not shown). It is surprising that the frequency of this band is nearly constant for this series (Table IV) since the pyrrole tilting mode might have been expected to be sensitive to the heme structure, especially to the out-of-plane

Table IV. RR Frequencies (cm^{-1}) below 600 cm^{-1} for PP Complexes and Myoglobin Derivatives

mode[a]	$Fe^{III}OEP$		$Fe^{III}PP$	$Fe^{II}PP$		$Fe^{III}PP$	$Fe^{II}PP$	myoglobin			frequency shift[b]			
	$(ImH)_2$	$(CN)_2$	$(ImH)_2$	$(ImH)_2$	$(CN)_2$	(Cl)	(2-MeImH)	Mb^{II}	$Mb^{III}F$	$Mb^{III}ImH$	$\Delta^{54}Fe$	Δd_α	$\Delta d_{2\beta}$	Δd_{4m}
$\nu_{Fe\text{-}Im}$							220	221			+3			
	228	236	236	237	228		243	220	216					
pyr tilt	225			254			255	255	251	255	2-3			
ν_9	276	267	276	263	267	266		270	273	273	1-2			
γC_mC_a	320		296	298	312	312	303	297	297	305				
$\delta C_bC_\alpha C_\beta(2)$			312	312	320	324	326	307	319	309			7	1-5
ν_8	345	349	349	345	346	345	345	342	345	346				2
$2\nu_{35}$			380			373			379	382				
γC_bS	359			384	372	380	374	373	335		1-2			
$\delta C_bC_\alpha C_\beta(1)$			419	412	412	415	410	408	412	412			10	
pyr fold	403	408	425	426	425	425								
pyr fold								441	442	438			10	5
pyr fold	469	466							472			10	10	
pyr fold			495	488	493	492	495	503[c]	501[c]	495		6		
pyr fold			510	507	512		510					6		
ν_{49} Eu			561	558	560	555	548	551	550	554		5		
ν_{48} Eu	580		605	588	588		585							

[a] Mode numbers and in-plane skeletal assignments follow Kitagawa et al.[7] [b] Frequency upshifts for ^{54}Fe, and downshifts for $-d_\alpha$, $d_{2\beta}$ and $-d_{4m}$ substitution. [c] May contain two pyrrole folding modes.

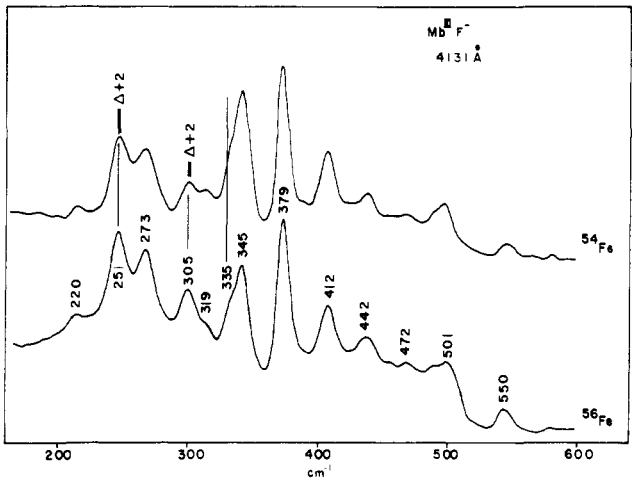

Figure 11. Low-frequency RR spectra (λ_0 = 4131 Å) of Mb^{III}F and Mb^{III}F reconstituted with ^{54}FePP, both in ~0.05 mM bis-tris buffer (0.025 M, pH 6.5). Spectral slit width, 5 cm^{-1}.

displacement of the Fe atom in (2-MeImH)Fe^{II}PP and Mb^{II}. The constancy may however be fortuitous. It is possible that the frequency is kept from decreasing in the out-of-plane structures by interaction with the nearby Fe–ImH stretching mode, at 205–220 cm^{-1}. Certainly the 1.5-cm^{-1} ^{15}N(pyrrole) shift observed[22] for the 204-cm^{-1} band of (2-MeIm)Fe^{II}EP implies appreciable N(pyrrole) movement in the mode and is consistent with substantial coupling between Fe–ImH stretching and pyrrole tilting coordinates. (A possible reversal of the 204- and 255-cm^{-1} band assignments, in view of their common ^{54}Fe and ^{15}N(pyrrole) sensitivities, can be rejected, since 2-MeImH perdeuteration affects only the lower frequency mode.[20]) In the case of Mb^{III}F, it cannot be excluded that the 255 cm^{-1} might instead arise from Fe–ImH stretching since this mode should also be ^{54}Fe sensitive (the two ligands being highly unequal in mass).

2. Methine Deformation. The 320-cm^{-1} band of (ImH)$_2$Fe^{II}OEP is assigned to the A_{2u} (in-phase) out-of-plane deformation of the methine carbon atoms, $\gamma_{C_aC_m}$, due to its substantial shift upon methine deuteration. The mechanism for the shift would be coupling with the 841-cm^{-1} γ_{C_mH} mode. The 1-cm^{-1} ^{54}Fe shift observed for a coincident IR band[24] suggests appreciable coupling as well to the 255-cm^{-1} pyrrole tilting mode. Most of the complexes in this study showed a d_4-sensitive band at 300–320 cm^{-1} and in some cases a ~1-cm^{-1} ^{54}Fe upshift could be detected. For PP complexes this region also contains the vinyl mode $\delta_{C_bC_aC_\beta(2)}$, but the two bands can frequently be resolved. As noted in section B, from the effects of C_m-d_4 and C_β-d_2 substitution, it appears that the higher of the two frequencies is $\delta_{C_bC_aC_\beta(2)}$ while the lower is $\gamma_{C_aC_m}$ (see Figures 3 and 14).

3. Peripheral Substituent Deformation. A logical candidate for the 359-cm^{-1} ^{54}Fe-sensitive band of [(ImH)$_2$Fe^{III}OEP]$^+$ would be the Fe–(ImH)$_2$ assymmetric stretch, but this mode has been assigned[25] to an intense 376-cm^{-1} ^{54}Fe-sensitive IR band, which does not appear in the RR spectrum. We assign the 359-cm^{-1} band to an A_{2u} mode involving the out-of-plane deformation of the peripheral ethyl groups (γ_{C_bS}). This motion should couple strongly with the tilting of the pyrrole rings (250 cm^{-1}) thereby accounting for the ^{54}Fe shift.

For [(ImH)$_2$Fe^{III}OEP]$^+$ the ^{54}Fe-sensitive band is superimposed on another band (seen as a shoulder in the [(CN)$_2$Fe^{III}OEP]$^-$ spectrum, Figure 7), assigned to $2\nu_{35}$, which is believed to be in Fermi resonance with ν_8, at 345 cm^{-1}.[g] This superposition complicates the interpretation of metalloporphyrin spectra in this region, especially because both the γ_{C_bS} mode and the Fermi-resonance interaction can be expected to produce bands of variable frequency and intensity. In the case of ClFe^{III}PP (Figure 12) two bands are clearly seen, at 373 and 380 cm^{-1}. The 380-cm^{-1} band shows a definite ^{54}Fe upshift, suggesting it to be γ_{C_bS} (the axial Fe–Cl mode being at 357 cm^{-1}),[25] while the unshifted 373-cm^{-1} band is assignable to $2\nu_{35}$. (ImH)$_2$Fe^{II}PP shows a single band

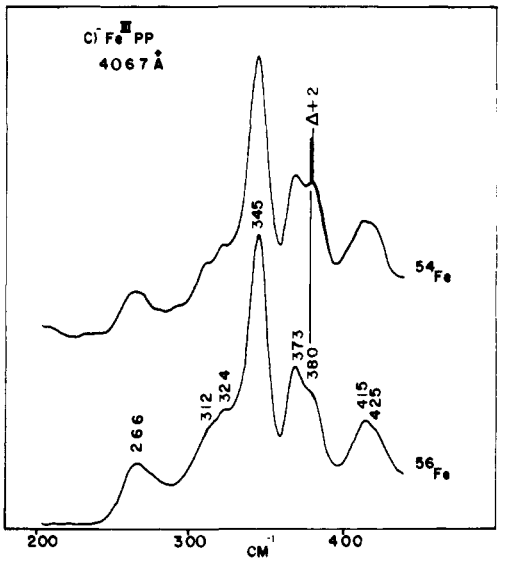

Figure 12. Low-frequency RR spectra (λ_0 = 4067 Å) of ClFe^{III}PP and its ^{54}Fe form, both in 20% (v/v) methanol/H$_2$O solution. Spectral slit width, 5 cm^{-1}.

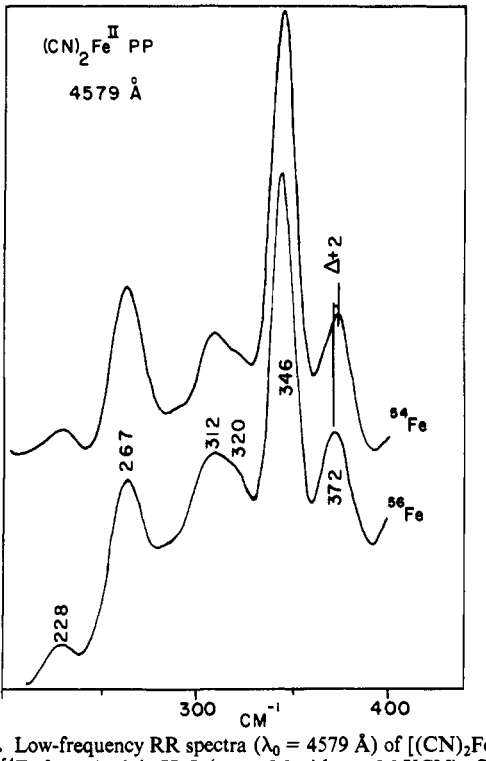

Figure 13. Low-frequency RR spectra (λ_0 = 4579 Å) of [(CN)$_2$Fe^{II}PP]$^{2-}$ and of its ^{54}Fe form, both in H$_2$O (~1 mM with ~1 M KCN). Spectral slit width, 5 cm^{-1}.

at 384 cm^{-1}, with an apparent 1-cm^{-1} upshift on ^{54}Fe substitution, suggesting it to be γ_{C_bS}; $2\nu_{35}$ is not seen. The higher γ_{C_bS} frequency, relative to [(ImH)$_2$Fe^{III}OEP]$^+$ may be due to the differing peripheral substituents in PP at OEP. In the cyanide analogue, [(CN)$_2$Fe^{II}PP]$^{2-}$ (Figure 13) a band appears at 372 cm^{-1}, which clearly shifts upon ^{54}Fe substitution. Thus, γ_{C_bS} appears to decrease by 10 cm^{-1} when CN$^-$ replaces ImH. Conceivably this is another manifestation of the nonbonded interaction between imidazole-H and pyrrole-N atoms, which might increase γ_{C_bS} via coupling with the pyrrole tilting mode. (We note that the latter mode is not observed for [(CN)$_2$Fe^{II}PP]$^{2-}$ but is observed at 255 cm^{-1} for (ImH)$_2$Fe^{II}PP, as expected. What is unexpected is that γ_{C_bS} is nevertheless activated for the cyanide complex; the mechanism for this activation is not understood.)

For both (2-MeImH)Fe^{II}PP (Figure 9) and Mb^{II} (Figure 10), γ_{C_bS} can be located at 373 cm^{-1}, via its ^{54}Fe sensitivity; again $2\nu_{35}$

is not seen, although it may underlie the 373-cm^{-1} band. Apparently the protein is without influence on the frequency of γ_{C_bS} in this case, although it is notable that the intensity of the band is much higher in Mb^{II} than in (2-MeImH)Fe^{II}PP.

A completely different pattern is seen for $Mb^{III}F^-$ (Figure 11). Here the strong and sharp band at 379 cm^{-1} shows no ^{54}Fe shift whatever, although ^{54}Fe-sensitive bands are observed at 251 cm^{-1} (pyrrole tilt) and 305 cm^{-1} ($\gamma_{C_aC_m}$). Since it is implausible that the protein could uncouple the modes sufficiently to cancel the ^{54}Fe shift, we infer that the 379-cm^{-1} band must arise from a different mode in $Mb^{III}F^-$ than in Mb^{II}. Presumably it is $2\nu_{35}$, (or ν_8, since the 373-cm^{-1} band is stronger than the 345-cm^{-1} band, the other partner in the presumed Fermi resonance). As for the location of γ_{C_bS}, we note that the $Mb^{III}F$ spectrum, in contrast to all the other heme spectra, has a prominent shoulder ($\sim$333 cm^{-1}) on the low-energy side of the 345-cm^{-1} band, and that this shoulder appears to shift further into the band upon ^{54}Fe substitution. Thus, the protein, in its $Mb^{III}F^-$ conformation, appears to shift γ_{C_bS} down by $\sim$40 cm^{-1} relative to Mb^{II}. An alternative and more plausible interpretation is that a different γ_{C_bS} mode is activated in $Mb^{III}F^-$ than in the other heme complexes; there are eight γ_{C_bS} modes, and all degeneracies and symmetry restrictions are lifted by the inequivaent PP substituents and by binding to the protein.

4. Pyrrole Folding Modes. The complex $(ImH)_2Fe^{II}$PP shows RR bands at 585, 557, 507, and 488 cm^{-1}, which shift down by 3–8 cm^{-1} upon vinyl C_α deuteration (Figure 3). The 585- and 557-cm^{-1} bands also shift, by 3 and 12 cm^{-1}, upon meso deuteration and correlate with the E_u modes ν_{48} and ν_{49},[8] appearing at 606 and 550 cm^{-1} in the IR spectrum of NiOEP[3] (and in the RR spectrum of the D_{2d} form of NiOEP,[18] Table I). These E_u modes, which are calculated[8] to involve angle bending within the pyrrole rings and at the C_b–substituent bonds, are evidently coupled to the vinyl groups. The 507- and 488-cm^{-1} bands, however, fall in a region where no in-plane modes are observed or calculated[8] for NiOEP but where pyrrole folding modes are expected.[30] Assignment of these bands to pyrrole folding is supported by the vinyl deuteration shifts, since coupling of pyrrole folding and vinyl out-of-plane C–H bending modes should be effective. There are three vinyl C–H out-of-plane modes, occurring in the 1000–600-cm^{-1} range, which shift down strongly on C_α or C_β deuteration.[9] The 507, 488 cm^{-1} pair of RR bands may arise from weakly coupled folding modes of the two vinyl-bearing pyrrole rings. All of the PP complexes studied show one or both of this pair of bands (Tables I and IV).

$(ImH)_2Fe^{II}$PP shows an additional, moderate intensity band at 426 cm^{-1}, where no in-plane mode is observed or calculated for NiOEP.[8] It is also seen for $[(CN)_2Fe^{II}PP]^{2-}$, $[(ImH)_2Fe^{III}PP]^+$, and $ClFe^{III}$PP. We tentatively assign it to a pyrrole folding mode which is not coupled to the vinyl groups (there is no C_α or C_β deuteration shift, Figure 3); presumably it is localized on the non-vinyl-bearing pyrrole rings. The peripherally symmetric OEP complex $[(ImH)_2Fe^{III}OEP]^+$ shows a moderately strong band at 469 cm^{-1} and a weak one at 403 (Figure 7); these are not seen for NiOEP.[7,9] They may likewise be pyrrole folding modes, activated by the axial ligands. These bands do not disappear, however, upon substitution of CN^- for ImH, in contrast to the 255- and 359-cm^{-1} out-of-plane modes. Their mechanism of activation is uncertain.

$Mb^{III}F^-$ shows three bands in the pyrrole folding region, at 442, 472, and 501 cm^{-1}, all of which shift down upon vinyl deuteration (Figure 14). The 501 cm^{-1} band is broad, and appears to contain two components. Very likely they correspond to the pair of vinyl-sensitive modes at 507 and 488 cm^{-1} in $(ImH)_2Fe^{II}$PP (Figure 3). The 472- and 442-cm^{-1} $Mb^{III}F^-$ bands then represent additional vinyl-sensitive modes. Since there are two kinds of pyrrole fold (Figure 5), the two vinyl-bearing pyrrole rings can give rise to a total of four folding modes, and it appears that all four are activated by the protein in $Mb^{III}F^-$. (They may, of course, include substantial contributions from the non-vinyl-bearing pyrroles; the degree of interpyrrole coupling for these modes is uncertain.) These bands can be expected to be sensitive monitors of the interactions between the porphyrin ring and the globin pocket.

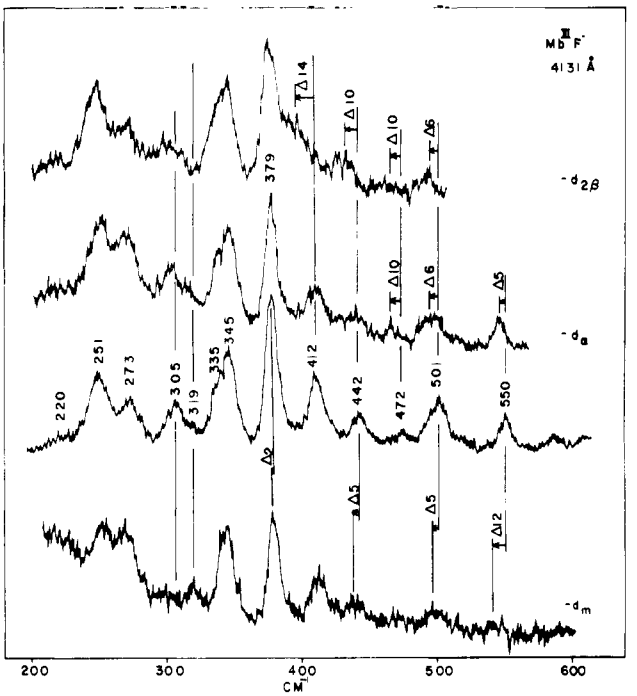

Figure 14. RR spectra of $Mb^{III}F$, showing the effects of deuteration at the vinyl C_β ($-d_{2\beta}$) or C_α ($-d_\alpha$) atoms, or at the meso carbon atoms ($-d_m$); conditions are the same as for Figure 11.

F. M–N(pyrrole) Stretching. Since the bonds from the central metal atom to the four pyrrole N atoms are of central importance in metalloporphyrin chemistry, there is naturally much interest in characterizing them via vibrational spectroscopy. Their contributions to the low-frequency bands of the RR spectra have frequently been speculated on, and Desbois and co-workers[22-24] have been particularly concerned to assign metal–pyrrole modes, using ^{54}Fe and ^{15}N (pyrrole) isotope shifts.

For a hypothetical *non*macrocyclic M(pyrrole)$_4$ complex, of D_{4h} symmetry, one would expect two M–pyrrole modes, A_{1g} and B_{1g}, at $\sim$250 cm^{-1}, by analogy with $Cu(ImH)_4^{2+}$,[37] and one IR mode, E_u, at a somewhat higher frequency (the pyrrole rings being more massive than the central metal atom, at least for the first transition row). Because, however, the pyrrole rings are part of the porphyrin macrocycle, the A_{1g} and B_{1g} M–pyrrole stretching coordinates are completely redundant with the ring deformation coordinates. The presence of the central metal atom adds *no* additional Raman modes to those of the porphyrin dianion. The M–N(pyrrole) stretching coordinates must, of course, contribute to the low-frequency modes, but they may be distributed into many of these. In the normal mode calculation of Abe et al.,[8] *none* of the A_{1g} modes shows a ν_{MN} contribution to the potential energy contribution in excess of 10%. The lowest frequency B_{1g} mode, calculated at 187 cm^{-1}, does show a 34% ν_{MN} contribution; it has not been assigned in the NiOEP RR spectra. Desbois et al.[23] assigned the 251-cm^{-1} RR band of $(ImH)_2Fe^{II}$EP to Fe–N(pyrrole) stretching, on the basis of the 1-cm^{-1} pyrrole–^{15}N shift, but, as discussed above, this shift is also expected for the pyrrole tilting assignment which is advanced in this work.

If M–N(pyrrole) stretching were a major contributor to any of the observed RR bands, then one would expect a systematic inverse relationship with the M–N bond length, which increases in the order Ni^{II}[38] < $(ImH)_2Fe^{II}$[35] < $(ImH_2)Fe^{II}$[39] < $(Me_2SO)_2Fe^{II}$[40] < $(Cl^-)Fe^{III}$[41] < (2-MeImH)Fe^{II}.[42] Examination

(37) Larrabee, J. A.; Spiro, T. G. *J. Am. Chem. Soc.* **1980**, *102*, 4217.
(38) Cullen, D. L.; Meyer, E. F., Jr. *J. Am. Chem. Soc.* **1974**, *96*, 2095.
(39) Radonovich, L. J.; Bloom, A.; Hoard, J. L. *J. Am.* Chem. *Soc.* **1972**, *94*, 2073.
(40) Mashicko, T.; Katsbern, M. G.; Spartalian, K.; Scheidt, R. W.; Reed, C. A. *J. Am. Chem. Soc.* **1978**, *100*, 6354.
(41) Hoard, J. L. *Science* (*Washington, D.C.*) **1971**, *174*, 215.

of the frequencies in Table I fails to reveal any such trend for any of the modes below 1000 cm^{-1}, in contrast to the porphyrin modes above 1450 cm^{-1}.[10,17,18] The band we identify with the lowest frequency A_{1g} mode, ν_9, ranges between 260 and 280 cm^{-1}, but there is no trend with the M–N distance (e.g., the $(Me_2SO)_2Fe^{III}$ frequency is higher than that of $(ImH)_2Fe^{III}$). Likewise the weak band near 230 cm^{-1}, which we assign to a B_{1g}, B_{2g}, or A_{2g} in-plane mode, shows a scatter of frequencies but no clear trend. Both of these bands are overlapped by the ~250-cm^{-1} pyrrole tilting mode, and their peak frequencies are difficult to determine reliably; it is conceivable that this uncertainty obscures an underlying trend. Nevertheless it is evident that the low-frequency RR spectra cannot readily be used as a monitor of the M–N(pyrrole) interaction.

Summary of Assignments

Because of the complexity of the low-frequency heme RR spectra, we illustrate in Figure 2 the assignments derived from this and previous[9] studies for NiPP and $(ImH)_2Fe^{II}PP$.

1. 1010–575 cm^{-1}. This region contains a number of in-plane porphyrin skeletal modes, which can readily be correlated with RR or IR modes of NiOEP. Several E_u modes are activated via the asymmetrically disposed vinyl groups of PP. In addition two out-of-plane hydrogenic modes are observed for $(ImH)_2Fe^{II}PP$: $\gamma_{CH=}$(vinyl) at 1008 cm^{-1} and γ_{C_mH} at 841 cm^{-1}.

2. 510–425 cm^{-1}. No in-plane modes occur in this region, but pyrrole folding modes are activated in $(ImH)_2Fe^{II}PP$ and in other iron complexes. Specific protein activation is seen for Mb derivatives.

3. 425–290 cm^{-1}. This region contains a cluster of bands of different types and of variable intensities in different complexes. The most prominent feature is usually the in-plane skeletal mode, ν_8, at ~345 cm^{-1}. It is usually accompanied by a mode at ~370 cm^{-1}, believed to be $2\nu_{35}$, in Fermi resonance with ν_8. At about the same frequency, however, is an out-of-plane mode, assigned here as γ_{C_bS}, coupled to the pyrrole folding mode at ~250 cm^{-1}, as evidenced by its ^{54}Fe shift. There are two flanking bands in PP complexes, assigned to vinyl bending modes, $\delta_{C_bC_aC_{\beta(1and2)}}$, at ~415 and ~320 cm^{-1}. Near, the latter band, at ~300 cm^{-1}, is another out-of-plane mode, $\gamma_{C_aC_m}$, involving the methine carbon atoms primarily.

4. 275–220 cm^{-1}. This region contains a cluster of at least three bands. In the middle, at ~250 cm^{-1}, is a ^{54}Fe- and ^{15}N(pyrrole)-sensitive band, assigned to pyrrole tilting. On either side, at ~260 and ~230 cm^{-1}, are bands assigned to in-plane skeletal modes, the higher of which is probably $\nu_9(A_g)$. While these bands can be expected to have some contribution from M–N stretching, their frequencies do no appear to correlate with the M–pyrrole distances.

Acknowledgment. This work was supported by NIH Grant HL 12526. We are indebted to Professor K. M. Smith for provision of vinyl-deuterated heme (supported by NIH Grant HL 22252) and to Professor G. N. La Mar for provision of Mb reconstituted with vinyl-deuterated heme (supported by NIH Grant HL 16087).

Registry No. $(ImH)_2Fe^{II}PP$, 85293-61-4; $(ImH)_2{}^{54}Fe^{II}PP$, 85282-43-5; $[(ImH)_2Fe^{III}OEP]Cl$, 85282-40-2; $[(ImH)_2{}^{54}Fe^{III}OEP]Cl$, 85293-64-7; $K[(CN)_2Fe^{IV}OEP]$, 85282-42-4; (2-MeImH)$Fe^{II}PP$, 85282-39-9; (2-MeImH)$^{54}Fe^{II}PP$, 85304-54-7; $ClFe^{III}PP$, 84009-29-0; $[(CN)_2Fe^{II}PP]^{2-}$, 85282-38-8; $[(CN)_2{}^{54}Fe^{II}PP]^{2-}$, 85304-53-6; NiPP, 85282-41-3.

(42) Hoard, J. L.; Scheidt, W. R. *Proc. Natl. Acad. Sci. U.S.A.* **1973**, *70*, 3919; **1974**, *70*, 1578.

Resonance Raman and Electronic Spectra of Heme *a* Complexes and Cytochrome Oxidase

S. Choi,† J. J. Lee,‡ Y. H. Wei,‡ and T. G. Spiro*†

Contribution from the Chemistry Departments, Princeton University, Princeton, New Jersey 08544, and State University of New York, Albany, New York 12222.
Received August 2, 1982

Abstract: Resonance Raman (RR) spectra of heme *a* complexes containing Fe^{II} and Fe^{III} in low- and high-spin states are assigned by comparison with protoheme analogues and by deuteration of the formyl substituent. Specific effects of the trans-conjugated formyl and vinyl groups include (a) RR enhancement of formyl and vinyl modes, (b) *x,y* splitting of the Q absorption bands by ~1600 cm^{-1}, (c) depolarization ratios near $^1/_3$ for most RR bands, (d) RR activation, and splitting, of E_u skeletal modes, with selective enhancements of the *x*- and *y*-polarized components, (e) skeletal mode shifts associated with the stabilization of one of the alternative 18-membered delocalization pathways of the porphyrin π system. For $(ImH)_2Fe^{II}Pa$ (ImH = imidazole, Pa = porphyrin *a*), increased Q-band splitting (~2000 cm^{-1}) and skeletal mode shifts are attributed to $d_\pi \rightarrow$ porphyrin π^* back-bonding; the formyl C=O stretching frequency is also lowered in this complex. For all complexes, the C=O frequency is lower in aqueous than in nonaqueous solutions, due to formyl H bonding. The skeletal frequencies above 1450 cm^{-1} correlate with porphyrin core size, as they do for protoheme complexes, and with the same slopes. Heme *a* aggregates in aqueous solution show no RR frequency changes, beyond the effects of H bonding, but display altered intensity patterns, attributable to the absorption wavelength changes and to altered excited-state distortions; striking intensity changes are seen for low-frequency bands assigned to out-of-plane deformations. The 4131-Å RR spectrum of oxidized cytochrome oxidase is dominated by heme a_3 while the 4545-Å spectrum of the reduced protein is dominated by heme *a*, although contributions from the remaining heme can be seen. In the oxidized form, the low-frequency RR spectrum is interpreted in terms of heme a_3 perturbed by protein–peripheral substituent interactions, instead of Cu^{2+} vibrations, as recently suggested; the heme a_3 skeletal frequencies are consistent with EXAFS results, indicating a long bond to the sixth ligand.

RR spectroscopy is being increasingly applied as a structure probe for heme proteins.[1] Cytochrome oxidase is an attractive subject for RR studies, and a number of spectra have been published[2-11] and discussed since the early report by Salmeen et al.[2] The protein complex contains two heme *a* molecules and two

† Princeton University.
‡ State University of New York.

(1) Spiro, T. G. In "The Chemical Physics of Biologically Important Inorganic Choromophores"; Lever, A. B. P., Gray, H. B., Eds.; Addison-Wesley: Reading, MA, in press.

0002-7863/83/1505-3692$01.50/0